

Modeling of a cable actuated elastica manipulator arm

F. C. Moon¹, E. S. Catto, and C. K. Yuan

¹ School of Mechanical and Aerospace Engineering, Cornell University, Ithaca, NY 14853, USA

Abstract

We present a unique manipulator called the Elasticarm. This robot arm is based on the elastica and uses a cable system to achieve three-dimensional motion with a single flexible beam. The Elasticarm has a parallel mechanism design and uses continuous beam deformations to perform tasks. The static shape of the arm is analyzed using large deformation beam theory. The workspace is calculated and an example of path planning is presented. The planar dynamics of the arm are modeled using a nonlinear finite element formulation. Linearizing this model, we demonstrate the dependence of the natural frequencies on the arm's configuration. The finite element results are validated with experimental results.

1 Introduction

The design of mechanisms and robot arms usually relies on the use of rigid structural elements. On the other hand, there are many situations where flexible elements have been useful. For example, the elastica has found utility in areas such as deployable structures (Miura 1993), compliant mechanisms (Howell and Midha 1995), and robot arms (Wilson and Mahajan 1989). The elastica may be regarded as a beam that admits large deflections without permanent deformation. As such, the elastica can assume very diverse three-dimensional configurations. Other features of elastica include low weight and the ability to store elastic energy.

In this paper we present a manipulator, which is based on the elastica, called the Elasticarm. This design was developed at Cornell University in four dissertations. Govindachar (1985) focused on the static analysis of the conceptual Elasticarm and verified his theoretical results using a simple experimental model. Yuan (1991) designed and constructed a prototype Elasticarm with servos and a computer interface. He also developed a preliminary dynamic model, performed dynamic testing, and implemented a simple control algorithm. Experimental results were presented on the robust control of the Elasticarm, where it was shown that direct strain feedback yields damping levels similar to a sophisticated H_∞ controller (Catto and Moon 1995).

The idea behind the Elasticarm is to exploit the flexibility of a beam so that three-dimensional end-effector positioning is obtained with a single beam element (without prismatic joints). As shown in Figure 1, the beam is held in a buckled state by a pair of cables. Motorized cable spools allow the cable lengths to be varied actively, which changes the beam shape. Conventional robot arms usually accomplish this type

of motion with an elbow. Thus we have removed the need for an elbow by exploiting the flexibility of a thin beam. The beam is clamped to a shoulder motor that is used to rotate the arm in its plane. The arm can also be rotated about the vertical axis with a base motor. Finally, the Elasticarm's end-effector is a gripper with a single wrist and parallel fingers.

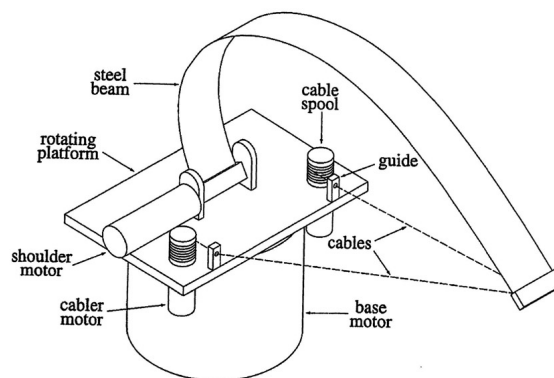


Figure 1: Diagram of the Elasticarm

In this paper we explore the planar statics and dynamics of the Elasticarm. To describe the statics we use nonlinear beam theory (Frish-Fay 1962; Love 1944) to develop the governing ordinary differential equation (ODE). Using this approach, Govindachar was able to obtain an explicit solution to the planar statics problem in terms of elliptic integrals. To obtain his solution he found it necessary to neglect the distributed weight of the arm. In this paper we include the distributed weight to achieve a higher degree of accuracy. Consequently, the increased complexity of the ODE prevents an elliptic integral solution, so we use a numerical approach. This approach is mathematically simpler than the elliptic integral solution and takes advantage of the speed and graphic capabilities of today's digital computers.

A dynamic model of the Elasticarm is developed using the finite element (FE) beam model (Simo and Vu-Quoc 1986). This model has the advantage of being fully nonlinear and geometrically exact. We use the FE model to predict the change in natural frequencies with the cable length, a measure that helps to demonstrate the nonlinearity of the Elasticarm. Finally, we present experimental results to verify the quality of the FE results.

2 Planar Statics

The geometry of conventional robot arms is governed by a set of nonlinear algebraic equations that are independent of the loads, since elastic deformations are typically ignored. Usually the desired end-effector position and orientation are specified and the joint angles are found either algebraically or numerically (Craig 2005). On the other hand, the geometry of the Elasticarm is governed by a set nonlinear differential equations that depend on the loading. However, the resulting boundary value problem can be posed as a set of nonlinear algebraic equations that can be solved numerically using standard root finding algorithms.

2.1 Formulation of the Governing ODE

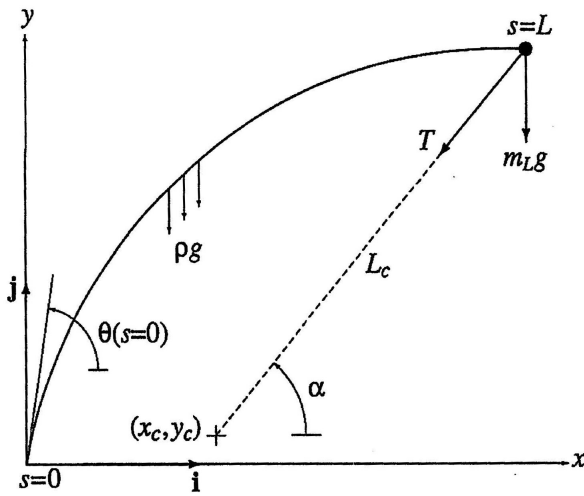


Figure 2: Setup for the planar problem

The setup for the planar problem is shown in Figure 2. The shoulder axle is clamped to the origin of the fixed frame i, j at an angle $\theta(0)$ and the beam's centerline is located by the coordinates $x(s), y(s)$. The beam has a length L and its arclength s is measured from the shoulder axle. The cable root is fixed at the point x_c, y_c . The beam's mass per unit length is given by p and the tip mass is given by m_L . The tip mass is the sum of the hand and payload mass

$$m_L = m_h + m_p \quad (1)$$

We assume both cables of the Elasticarm have equal lengths and, therefore, imagine a equivalent central cable with length L_c . The cable tension T is directed towards the cable root at an angle α . The gravitational field acts in the negative j direction. In the ODE analysis we take the beam to be inextensible, unshearable, and linearly elastic. As well, the cables are assumed to be straight, inextensible, and to support no moment. By considering an arbitrary position along the beam, we write the internal force acting on a cross section as

$$P(s) = N(s)t(s) + Q(s)n(s) \quad (2)$$

where N and Q are the axial and shear force, respectively. The local frame t, n is related to the fixed frame by the transformation

$$\begin{Bmatrix} t(s) \\ n(s) \end{Bmatrix} = \begin{bmatrix} \cos \theta(s) & \sin \theta(s) \\ -\sin \theta(s) & \cos \theta(s) \end{bmatrix} \begin{Bmatrix} i \\ j \end{Bmatrix} \quad (3)$$

where θ is the rotation of the centerline. Using an elementary force balance and equation (3) yields

$$N = -[m_L + p(L-s)]g \sin \theta - T \cos(\theta - \alpha) \quad (4)$$

$$Q = -[m_L + p(L-s)]g \cos \theta + T \sin(\theta - \alpha) \quad (5)$$

By considering a differential element of the beam, we obtain the moment balance

$$Q = -\frac{dM}{ds} \quad (6)$$

and the differential relationships

$$\frac{dx}{ds} = \cos \theta \quad (7)$$

$$\frac{dy}{ds} = \sin \theta \quad (8)$$

where M is the bending moment. We now make the standard constitutive assumption that the bending moment is linearly proportional to the curvature

$$M = EI \frac{d\theta}{ds} \quad (9)$$

where EI is the flexural rigidity of the beam. Using equations (5) and (6), we obtain the governing ODE

$$EI \frac{d^2\theta}{ds^2} - [m_L + p(L-s)]g \cos \theta + T \sin(\theta - \alpha) = 0 \quad (10)$$

Due to the explicit appearance of the arclength s , equation (10) does not admit a solution in terms of elliptic integrals (Frish-Fay 1962). It is convenient to arrange equations (7), (8), and (10) into the state-space form

$$\frac{d}{ds} \begin{Bmatrix} \theta \\ \kappa \\ x \\ y \end{Bmatrix} = \begin{Bmatrix} \kappa \\ [m_L + p(L-s)]g \cos \theta - T \sin(\theta - \alpha) \\ \cos \theta \\ \sin \theta \end{Bmatrix} \quad (11)$$

where $k := \theta'$ denotes the curvature and $(\cdot)' := d(\cdot)/ds$. The cable tension T and the cable angle α vary with the arm's configuration and must be prescribed or determined as part of the solution.

2.2 Numerical Solution Procedure

As stated previously, equation (11) contains s explicitly (due to the distributed weight of the arm) so that a solution in terms of elliptic integrals is not possible; therefore, we solve equation (11) using numerical integration combined with a root finding algorithm. It is important to note that the arm configuration can be specified in many different ways. For

example, if the coordinates of the tip are given, then α may be calculated directly as

$$\tan \alpha = \frac{y_L - y_c}{x_L - x_c} \quad (12)$$

while T , θ_0 , and κ_0 must be solved for numerically. Likewise, T and θ_0 may be specified while κ_0 and α must be solved for numerically. It is useful to consider the governing ODE as a function which maps the shoulder boundary conditions, cable tension, and cable angle to the tip boundary conditions. Therefore, we define a function h such that

$$\hat{x}(L) := h(\alpha, T, \theta_0, \kappa_0) \quad (13)$$

Where $\hat{x}(L)$ is the calculated state at the tip rather the desired state. Given the arguments of h , some of which may be specified while the others are guesses, we may numerically integrate equation (11) as an initial value problem to obtain $\hat{x}(L)$. If the calculated values do not match the specified values, it is necessary to iterate the unknown arguments of h until a solution is achieved. Note that often $\hat{x}(L)$ is only partially specified while the remaining terms are merely by-products of the solution. For example, θ_L is rarely specified. Our procedure is similar to the shooting method. In a linear boundary value problem the shooting method yields a solution after two iterations and one extrapolation (Press et al. 1988). However, equation (11) is a nonlinear ODE, so the shooting method becomes entirely iterative. Fortunately, the problem may be posed as set of nonlinear algebraic equations whose roots yield the unknowns. The equations express requirements on $\hat{x}(L)$ and may be stated in the form

$$g(\hat{x}(L)) = 0 \quad (14)$$

The function g represents specifications on the tip boundary conditions, which vary between different statements of the statics problem. Equation (14) may be further refined by defining

$$g^*(\alpha, T, \theta_0, \kappa_0) =: g[h(\alpha, T, \theta_0, \kappa_0)] = 0 \quad (15)$$

Standard software packages are capable of solving the types of equations numerically. Of course, since the equations are nonlinear, multiple solutions are possible.

2.3 Examples

We now present three examples that illustrate the numerical solution procedure and help to characterize the operation of the Elasticarm. We use the parameter values as given in Table 1.

2.3.1 Manipulator Workspace

In this example we investigate the workspace of the Elasticarm. The Elasticarm is highly deformable, so the payload has a significant effect on the extent of the

Table 1: Arm parameter values

ρ	0.501 kg/m
m_h	0.230 kg
L	0.914 m
EI	0.705 Nm ²
x_c	0.098 m
y_c	-0.006 m

workspace. In the following we define the Elasticarm's workspace and show the effect of the payload m_p on the extent of the workspace. The extent of the Elasticarm's reach is indicated by zero cable tension. To calculate the arm's reach we set $T = 0$ and specify a value for the cable angle α . The remaining unknowns are θ_0 and κ_0 . To find these unknowns we must make two requirements on the tip boundary conditions. These requirements are given by

$$g^*(\theta_0, \kappa_0) := \left\{ \begin{array}{l} \hat{\kappa}_L(\theta_0, \kappa_0) \\ \tan \alpha - (\hat{y}_L(\theta_0, \kappa_0) - y_c) / (\hat{x}_L(\theta_0, \kappa_0) - x_c) \end{array} \right\} = 0 \quad (16)$$

where we use a hat to indicate a calculated value. These conditions state that the tip moment must be zero and the tip coordinates must be compatible with the specified cable angle.

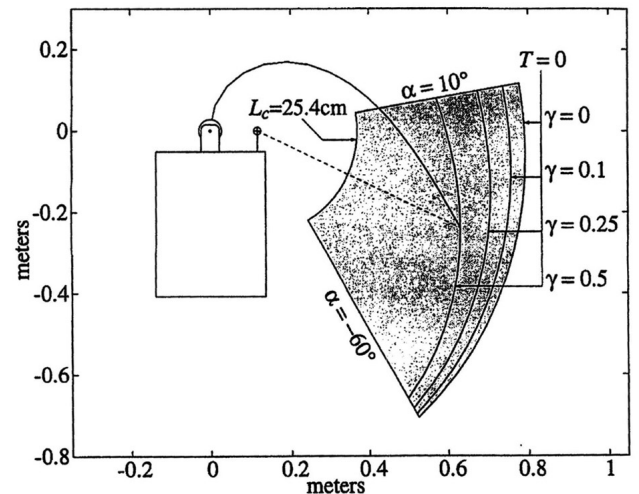


Figure 3: Workspace for various values of the payload factor γ .

Figure 3 shows the workspace that we have defined along with the effect of payload variation. The outer edge of the workspace is found by setting the cable tension to zero and sweeping the cable angle between -60 and 10 . A sequence of edges are found by varying the payload as a fraction of combined arm and hand mass using

$$m_p = \gamma(m_h + \rho L) \quad (17)$$

where ρ is defined as the payload factor. Figure 4 shows the tip traces for $\rho = 0, 0.1, 0.25, 0.5$. The inner edge of the workspace is determined by limiting the cable length to 25.4 centimeters.

2.3.2 Torque Scheduling

The Elasticarm is equipped with sensors to measure the cable length L_c , the cable angle α , and the base angle. Through

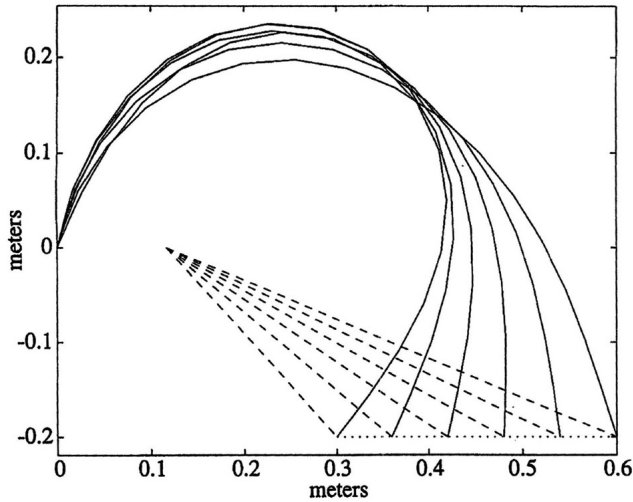


Figure 4: Path planning of straight line tip motion

the use of feedback, this allows one to specify the tip position in terms of spherical coordinates. With this setup it is useful to know the shoulder motor torque required to compensate the gravitational and cable loads in terms of L_c , and α .

2.3.3 Path Planning

The final example of the ODE model demonstrates the Elasticarm's ability to follow operator-defined tip paths. We choose the straight line path defined by

$$x_d(\beta) := 0.3\beta + 0.3\text{meters} \quad y_d(\beta) := -0.2\text{meters} \quad (18)$$

where $(\cdot)_d$ denotes the desired path and $\beta \in [0,1]$ is used to parameterize the tip path. The cable length and cable angle are calculate according to

$$L_c(\beta) = [(x_d(\beta) - x_c)^2 + (y_d(\beta) - y_c)^2]^{1/2} \quad (19)$$

$$\alpha(\beta) = \tan^{-1} \frac{y_d(\beta) - y_c}{x_d(\beta) - x_c} \quad (20)$$

Figure 4 shows the solution for six steps in 0. Note that such a solution is not necessary for path planning if the arm is equipped with sensors to measure L_c and α , so that an arbitrary path can be generated with equations like (19) and (20). In other words, it is not necessary to know the elastic curve to generate trajectories. However, the static solution is useful for determining if a path is *admissible*. An indication of an inadmissible path is a negative cable tension or, at worst, the lack of a solution.

3 Finite Element Model

Since the beam of the Elasticarm experiences very large deflections and rotations, it is necessary to use a fully nonlinear FE (finite element) model. We use a geometrically exact beam element (Simo and Vu-Quoc 1986). This element

is planar and includes the effects of shear strain and axial extension as well as flexure. Even though the Elasticarm experiences negligible shear and extension, it is simpler to include the degrees of freedom in the dynamic model because the constraint equations, found by setting shear and extension to zero, are differential and lead to spatial integrals in the inertia terms. Unlike Simo and Vu-Quoc who use a Galerkin approach, we use a virtual work formulation to derive the element model. Of course, both approaches yield identical results.

3.1 Cable Element Formulation

The manner in which the cable system is modeled depends on whether the cable length or tension is prescribed. To simulate the actuation of the cable spools we specify the cable tension rather than the cable length. In this case the elastic nature of the cable may be neglected and the cable loading on the arm tip is treated as a force of known magnitude that is directed at the cable guide. We refer to this situation as the active phase. We use the active phase for solving the statics problem, although dynamic problems may also be solved given a time history for the cable tension. The other mode of operation is referred to as the passive phase. In this phase the reference cable length is fixed while the cable tension has contributions from the static tension and the elastic response of the cable. The passive phase is used to analyze the local dynamics about a given static solution.

3.2 Static Solution

Let us consider the static problem

$$P_G(q_G) = F_G(q_G) \quad (21)$$

This problem is solved in the active phase using results from the ODE analysis, which include the displacement field q_G^0 and the cable tension T^0 . Due to the differences between the ODE and FE models, we should anticipate that q_G^0 is not an equilibrium solution for the FE model, but rather we take it as an initial guess for Newton-Rasphon iteration,

$$q_G^{i+1} = q_G^i + K_G^{-1}(q_G^i)[P_G(q_G^i) - F_G(q_G^i)] \quad (22)$$

where i is the iteration number. We measure the convergence of equation (22) with the formula

$$\epsilon^i = \frac{\|P_G(q_G^i) - F_G(q_G^i)\|}{\|F_G(q_G^i)\|} \quad (23)$$

In our simulations we terminate iterations when $\epsilon^i \leq 10^{-6}$. Table 2 gives the additional parameters used in the FE formulation.

Table 2: Additional parameter values.

EA	$1.28 \times 10^8 \text{ N}$
βGA	$3.28 \times 10^6 \text{ N kg}$
EA_c	$1.02 \times 10^5 \text{ N}$
I_{zz}	$2.68 \times 10^{-8} \text{ kg} \cdot \text{m}$
I_L	$4.00 \times 10^{-4} \text{ kg} \cdot \text{m}^2$

3.3 Frequencies of vibration

We characterize the nonlinearity of the Elasticarm by calculating the variation of the natural frequencies as the cable length varies. The frequencies of vibration are measured about a static solution, from the active phase, by putting the FE model into the passive phase. The cable length is varied by using a sequence of static solutions. At a particular static solution q_G we calculate the natural frequencies by solving the eigenvalue problem

$$(K_G(q_G) - \omega^2 M_G)v = 0 \quad (24)$$

where ω is the natural frequency and v is the corresponding mode shape. Figure 5 shows the first three frequencies of vibration versus cable length along with typical mode shapes. For this analysis we kept the cable angle at 0 and varied the cable length between 25.4 and 63.5 centimeters. The FE model consists of six quadratic elements and uses reduced order Gaussian integration to prevent shear locking (Simo and Vu-Quoc 1986). Experimental results included in Figure 5 agree well with our calculations. The first natural frequency increases 55% as the cable length is decreased, while the second and third natural frequencies increase by 38% and 12%, respectively, as the cable length is increased.

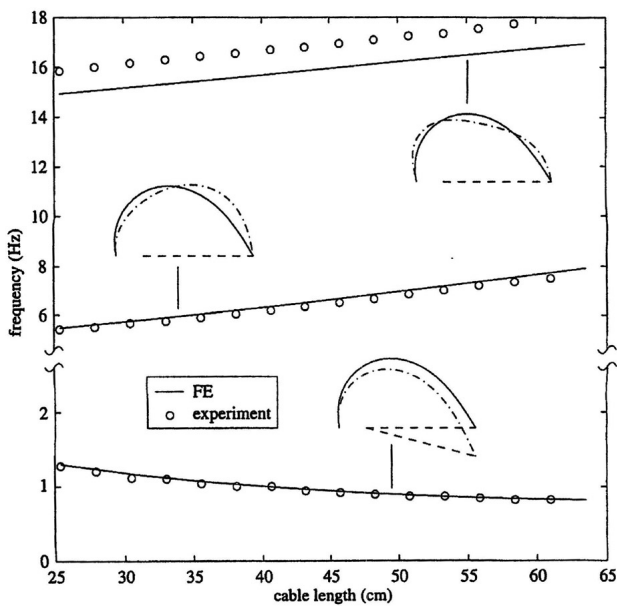


Figure 5: Variation of natural frequencies with cable length for $\alpha = 0^0$

4 Conclusion

We presented a unique manipulator design that exploits the flexibility of a thin beam by inducing a shape changing behavior with an actuated cable system. We have developed a numerical procedure for calculating the static shape of the arm. This procedure is more general than the usual elliptic integral approach because it allows for distributed loads. A

fully nonlinear finite element model was developed to analyze the planar dynamics. We characterized the nonlinearity of the arm by investigating the variation of the natural frequencies with the cable length. These results can be important in formulating control strategies that enhance damping across a range of natural frequencies.

1. Catto, E. S. and F. C. Moon (1995, March). Robust control of a shape-changing flexible robot arm. In I. Chopra (Ed.), *Smart Structures and Materials 1995: Smart Structures and Integrated Systems*, Volume 2443, San Diego, pp. 171-181. SPIE.
2. Cook, R. D., D. S. Malkus, and M. E. Plesha (1989). *Concepts and Applications of Finite Element Analysis* (3rd ed.). John Wiley & Sons, Inc.
3. Craig, J. J. (2005). *Introduction to Robotics*. Addison-Wesley. 3rd Edition
4. Frish-Fay, R. (1962). *Flexible Bars*. Butterworths.
5. Govindachar, S. (1985). Elasticarm: A continuous beam manipulator. Master's thesis, Cornell University, Department of Theoretical and Applied Mechanics.
6. Howell, L. L. and A. Midha (1995). Parametric deflection approximations for end-loaded, large-deflection beams in compliant mechanisms. *Journal of Mechanical Design* 117, 156-165.
7. Love, A. E. H. (1944). *A Treatise on the Mathematical Theory of Elasticity*. Dover.
8. Miura, K. (1993). Concepts of deployable space structures. *International Journal of Space Structures* 8(1-2), 1-16.
9. Press, W. H. et al. (1988). *Numerical Recipes in C*. Cambridge University Press.
10. Ringe, R.S. (2001). Mechanics of the backward reach of a cable actuated elastica manipulator arm. M.S. Dissertation, Cornell University, 2001
11. Simo, J. C. and L. Vu-Quoc (1986). On the dynamics of flexible beams under large overall motions-the plane case: parts i & ii. *Journal of Applied Mechanics* 53, 849-863.
12. Thomson, W. T. (1988). *Theory of Vibration with Applications* (3rd ed.). Prentice-Hall.
13. Wilson, J. F. and U. Mahajan (1989). The mechanics and positioning of highly flexible manipulator limbs. *Journal of Mechanisms, Transmissions, and Automation in Design* 111, 232-237
14. Yuan, C. K. (1991). The Statics, Dynamics and Control of the Elasticarm: A Continuous Beam Manipulator. Ph. D. thesis, Cornell University, Department of Mechanical and Aerospace Engineering.

